CDC50 Proteins Are Critical Components of the Human Class-1 P$_4$-ATPase Transport Machinery*

Susanne Bryde[‡§1,2], **Hanka Hennrich**[‡1,2], **Patricia M. Verhulst**[‡1], **Philippe F. Devaux**[§], **Guillaume Lenoir**[¶‖], and **Joost C. M. Holthuis**[‡3]

From the ‡Department of Membrane Enzymology, Bijvoet Center and Institute of Biomembranes, Utrecht University, 3584CH Utrecht, the Netherlands, the §Institut de Biologie Physico-Chimique, UMR CNRS 7099, Paris, France, the ¶CEA, iBiTecS Institut de Biologie et Technologie de Saclay and CNRS, URA 2096 Systèmes Membranaires, Photobiologie, Stress et Détoxication, F-91191 Gif-sur-Yvette, France, and the ‖Univ Paris-Sud 11, F-91405 Orsay, France

Members of the P$_4$ subfamily of P-type ATPases catalyze phospholipid transport and create membrane lipid asymmetry in late secretory and endocytic compartments. P-type ATPases usually pump small cations and the transport mechanism involved appears conserved throughout the family. How this mechanism is adapted to flip phospholipids remains to be established. P$_4$-ATPases form heteromeric complexes with CDC50 proteins. Dissociation of the yeast P$_4$-ATPase Drs2p from its binding partner Cdc50p disrupts catalytic activity (Lenoir, G., Williamson, P., Puts, C. F., and Holthuis, J. C. (2009) J. Biol. Chem. 284, 17956–17967), suggesting that CDC50 subunits play an intimate role in the mechanism of transport by P$_4$-ATPases. The human genome encodes 14 P$_4$-ATPases while only three human CDC50 homologues have been identified. This implies that each human CDC50 protein interacts with multiple P$_4$-ATPases or, alternatively, that some human P$_4$-ATPases function without a CDC50 binding partner. Here we show that human CDC50 proteins each bind multiple class-1 P$_4$-ATPases, and that in all cases examined, association with a CDC50 subunit is required for P$_4$-ATPase export from the ER. Moreover, we find that phosphorylation of the catalytically important Asp residue in human P$_4$-ATPases ATP8B1 and ATP8B2 is critically dependent on their CDC50 subunit. These results indicate that CDC50 proteins are integral part of the P$_4$-ATPase flippase machinery.

In eukaryotic cells, the plasma membrane as well as membranes of late secretory and endocytic compartments display asymmetric lipid distributions with the aminophospholipids phosphatidylserine (PS)[4] and phosphatidylethanolamine (PE) concentrated in the cytosolic leaflet (1–3). Maintenance of this lipid asymmetry has been implicated in membrane bending and the biogenesis of endocytic and secretory vesicles (4–

6), while its regulated dissipation is associated with a multitude of (patho)physiological processes, including blood coagulation, sperm capacitation, myoblast fusion, virus entry into host cells, and phagocytic clearance of apoptotic bodies (7–9). Consequently, defining the mechanisms responsible for creating lipid asymmetry and their functional implications has become an active area of research.

A widely held concept is that lipid asymmetry is generated and maintained by ATP-fuelled translocases that catalyze unidirectional transport of phospholipids across the bilayer (10, 11). A prime example is the aminophospholipid translocase in red blood cells that mediates a rapid transport of PS and PE from the exoplasmic to the cytosolic leaflet of the membrane (12). Similar activities operate at the plasma membrane (13), in the trans-Golgi network (14) and in post-Golgi secretory vesicles of nucleated cells (2, 15). Purification and subsequent cloning of a Mg^{2+}-ATPase associated with aminophospholipid translocase activity in bovine chromaffin granules resulted in identification of the P$_4$ subfamily of P-type ATPases (16). Subsequent work in yeast (2, 5, 14), Arabidopsis (17, 18), Caenorhabditis elegans (19), and mammals (20, 21) revealed that P$_4$-ATPases are indeed required for sustaining aminophospholipid transport and asymmetry while two recent studies demonstrated the reconstitution of aminophospholipid translocase activity with a purified P$_4$-ATPase (22, 23).

P-type ATPases usually pump small cations or metal ions. Besides P$_4$-ATPases, the superfamily of P-type pumps includes soft-transitional metal-transporting ATPases (P$_1$), Ca^{2+}-ATPases (P$_{2A/B}$), Na$^+$/K$^+$-ATPases, and H$^+$/K$^+$-ATPases (P$_{2C}$), and H$^+$-ATPases (P$_3$) (24). Transport is accomplished by cycling changes between two main enzyme conformations, E_1 and E_2, during which the ATPase is transiently phosphorylated by ATP at an invariant aspartate residue (hence the designation P-type). This arrangement allows for a controlled opening and closing of cytoplasmic and exoplasmic pathways that give access to the cation-binding sites, which are buried inside the membrane-spanning region of the pump (25). High-resolution x-ray structures of sarcoplasmic reticulum Ca^{2+}-ATPase (26, 27), Na$^+$/K$^+$-ATPase (28, 29), and H$^+$-ATPase (30) in well-defined states of the reaction cycle revealed similar structural elements and that the transport mechanism rests on common principles for these pumps. Differences are largely confined to the cation-binding pocket, which consists of a congregation of glutamates and aspartates

TABLE 1
RT-PCR primer sequences

mRNA	Forward primer sequence	Reverse primer sequence
ATP8A1	5′-acatgttgaagtaccctgaat-3′	5′-aaaagcagtcctcttgataacct-3′
ATP8A2	5′-gtcactgcatcaacgccttgg-3′	5′-ttgctatcccgcagcaccgcttt-3′
ATP8B1	5′-gttgctgtgtgcttactacc-3′	5′-tcagctgtccccggtgc-3′
ATP8B2	5′-gggctcttcgacatgtttc-3′	5′-gccaacccgccgcatgcagcg-3′
ATP8B3	5′-agtatcccccacgaccttc-3′	5′-tgggctcgaagctgcctc-3′
ATP8B4	5′-gccttggataccagttactg-3′	5′-gctaaagctgctcacggtg-3′
CDC50A	5′-atggcgatgaactataacg-3′	5′-aatggtaatgtcagctgtattac-3′
CDC50B	5′-tgaggcccacaaattacctg-3′	5′-ataaactggtaagatgatatcac-3′
CDC50C	5′-atggaggagagagcacagc-3′	5′-gcactttgatttgtacagatga-3′

whose anionic carboxyl groups serve to neutralize the charge of the cations. In P$_4$-ATPases, these anionic residues have been largely replaced by a mixture of hydrophobic and polar uncharged residues (16, 31). Yet how the conserved mechanism of P-type ATPase-mediated cation transport is adapted in P$_4$-ATPases to flip phospholipids is not understood.

P$_4$-ATPases form heteromeric complexes with members of the CDC50 protein family (32, 33). CDC50 proteins consist of two membrane spans and a large exoplasmic loop, which is stabilized by one or more disulfide bonds. Mutation of *CDC50* genes in yeast and *Arabidopsis* has been shown to phenocopy P$_4$-ATPase mutations and disrupt aminophospholipid transport and asymmetry (18, 32, 34, 35). Presumably, this is because assembly of a P$_4$-ATPase/CDC50 complex is a prerequisite for P$_4$-ATPase export from the endoplasmic reticulum (ER)(18,32,33,36). Human ATP8B1, a P$_4$-ATPase linked to familial intrahepatic cholestasis or Byler disease (37), requires a CDC50 homologue for ER export and delivery to the plasma membrane (38). Whereas these studies clearly demonstrate that CDC50 proteins are indispensable for proper intracellular targeting of P$_4$-ATPases, they do not address whether CDC50 proteins also contribute to the transport properties of the complex. An intimate role for CDC50 proteins in P$_4$-ATPase-catalyzed phospholipid transport can be inferred from our recent finding that dissociation of the yeast P$_4$-ATPase Drs2p from its binding partner Cdc50p disrupts the ability of the enzyme to form a phosphoenzyme intermediate (39). Using a genetic reporter system, we also found that the affinity of Drs2p for Cdc50p fluctuates during the reaction cycle with the strongest interaction occurring at or near a point where the enzyme is loaded with phospholipid ligand (39). Together, these results suggest that CDC50 proteins play a critical role in the P$_4$-ATPase transport reaction.

Yeast contains three CDC50 homologues on five P$_4$-ATPases (32) while *Arabidopsis* has five CDC50 homologues on 12 P$_4$-ATPases (18, 36). Most strikingly, the human genome encodes only three CDC50 homologues on a total of 14 different P$_4$-ATPases (40). In addition, expression of one of the CDC50 homologues, CDC50C, is restricted to testis (41). This implies that each human CDC50 protein interacts with multiple P$_4$-ATPases or, alternatively, that some human P$_4$-ATPases function alone. To gain further insight into the role of CDC50 proteins in P$_4$-ATPase-catalyzed phospholipid transport, we here set out to systematically map physical and functional interactions between human class-1 P$_4$-ATPase and CDC50 family members.

EXPERIMENTAL PROCEDURES

Cell Culture—HeLa and Caco-2 cells were grown in Dulbecco's modified Eagle's medium (PAA Laboratories GmbH, Colbe, Germany) supplemented with 10% fetal calf serum (Invitrogen) under 5% CO_2 at 37 °C. UPS-1 cells (a kind gift of K. Hanada, National Institute of Infectious Diseases, Tokyo, Japan) were grown in Ham's F12 Medium (Invitrogen, Leek, the Netherlands) supplemented with 5% fetal calf serum under 5% CO_2 at 32 °C. Sf9 insect cells were grown in InsectXpress Medium supplemented with 5% fetal bovine serum (Lonza Ltd, Basel, Switzerland) at 27 °C.

Cloning and Expression of Epitope-tagged Proteins—Commercially available cDNAs (RZPD, Berlin, Germany; Kazusa DNA Research Institute, Chiba, Japan; NITE, Chiba, Japan; JCRB, Tokyo, Japan) were used as templates to PCR amplify and subclone the open reading frames of human ATP8B1, ATP8B2, ATP8B4, CDC50A, CDC50B, and macaque CDC50C into pcDNA3.1 (Invitrogen). A full-length cDNA of ATP8A1 was kindly provided by L. Klomp (UMC Utrecht, the Netherlands). A triple HA (HA$_3$) and polyhistidine (His$_8$ or His$_{10}$) tag or a HA$_3$ and monomeric red fluorescent protein (mRFP) tag was added to the C terminus of the P$_4$-ATPases while a V5-tag was added to the C terminus of the CDC50 subunits by fusion PCR. Enzymatically inactive P$_4$-ATPases with a single point mutation replacing the phosphorylatable aspartate residue were created by side-directed mutagenesis (Stratagene) based on the manufacturer's protocol. HeLa and UPS-1 cells were transfected with the resulting plasmids using Lipofectamine2000 (Invitrogen) or Effectene (Qiagen) according to instructions of the manufacturer.

RT-PCR—To differentiate between cDNA and genomic DNA, primers were designed at distinct sites of the exon-exon boundaries (Table 1). P$_4$-ATPase primers were all chosen in the C-terminal tail, which displays the highest sequence variation. CDC50B primers match sequences in the 3′-UTR around the single exon-exon boundary present in the transcript. HeLa and Caco-2 cells were grown confluent in 10 cm ø dishes. RNA was isolated using Trizol Reagent (Invitrogen) and RT-PCR was performed using the Titan One Tube RT-PCR System (Roche Diagnostics BV, Almere, the Netherlands). To verify CDC50B primers, PCR was performed on genomic DNA of HeLa and Caco-2 cells by omitting the RT-step of the Titan One Tube RT-PCR protocol and starting with an extra 2 min at 94 °C.

Immunofluorescence Microscopy—HeLa and UPS-1 cells were grown on glass coverslips to 50% confluency and trans-

fected with different P$_4$-ATPases and/or CDC50 expression constructs using Lipofectamine 2000 (Invitrogen) or Effectene (Qiagen). Cells were grown for another 3 days. Prior to chemical fixation with 3% paraformaldehyde, protein expression was induced for 10–16 h with 1 mM sodium butyrate. Fixed cells were permeabilized with saponin and stained with mouse anti-V5 antibody (Invitrogen), rabbit anti-V5 antibody (Sigma-Aldrich), FITC-conjugated rat anti-HA antibody (Roche Diagnostics B.V.), rabbit anti-PDI (kindly provided by I. Braakman, Utrecht University, the Netherlands) or mouse anti-FTCD (Sigma-Aldrich). Texas Red conjugated goat anti-rabbit, Texas Red conjugated goat anti-mouse, FITC-conjugated goat anti-rabbit (Jackson Brunschwig, Amsterdam, the Netherlands), Alexa Fluor 488 or 568 conjugated goat anti-mouse and goat anti-rabbit antibodies (Invitrogen) were used as secondary antibody. A Nikon D-eclipse C1 confocal microscope was used for capturing images.

Immunoprecipitation—HeLa cells were transfected with different combinations of P$_4$-ATPase and CDC50 expression constructs using Lipofectamine 2000 (Invitrogen) and grown for another 3 days. Prior to cell lysis, protein expression was induced for 10–16 h with 1 mM sodium butyrate. Cells were scraped in ice-cold PBS$^+$ (PBS, 0.9 mM CaCl$_2$, 0.5 mM MgCl$_2$, 1 mM PMSF) containing protease inhibitors (1 μg/ml apoprotein, 1 μg/ml leupeptin, 1 μg/ml pepstatin, 5 μg/ml antipain, 157 μg/ml benzamidine), and solubilized at 4 °C for 1 h with 1% digitonin dissolved in PBS$^+$. The extract was cleared of cell debris and insoluble material by two subsequent centrifugation steps (18,000 $\times$ g, 10 min, 4 °C and 100,000 $\times$ g, 30 min, 4 °C). In the presence of 0.2% BSA, the solubilized fraction was incubated at 4 °C for 16 h with anti-V5-agarose affinity beads (Sigma-Aldrich). After washing, beads were incubated at 48 °C for 5 min with SDS/urea sample buffer containing protease inhibitors, and the supernatant was subjected to SDS gel electrophoresis and immunoblotting using rabbit anti-V5 (Sigma-Aldrich), rabbit anti-HA (Santa Cruz, Heerhugowaard, the Netherlands), and rabbit anti-ATP1A1 antibody (C356-M09, kindly provided by J. Koenderink, Radboud University, Nijmegen, The Netherlands).

Preparation of Baculovirus Stocks—Baculovirus stocks for heterologous expression of human ATP8B1, ATP8B1^{D454N}, ATP8B2, ATP8B2^{D425N}, and CDC50A were generated using the BAC-to-BAC system (Invitrogen). HA$_3$/His$_{10}$-tagged P$_4$-ATPases and V5-tagged CDC50A were subcloned into pFastBacDual plasmids. Viral DNA was prepared following the BAC-to-BAC system manual. Viral stocks were prepared according to protocols obtained from R. Callaghan (Oxford University, UK). In brief, Sf9 cells were transfected with bacmid DNA using Cellfectin (Invitrogen). 5–7 days post-transfection, culture medium containing virus particles was harvested and subjected to a plaque assay to subclone obtained viral particles. The ensuing viral supernatants were amplified in three successive infection steps with a multiplicity of infection (MOI) of 0.1 to obtain a viral working stock for large-scale infections. Viral supernatants were stored protected from light at 4 °C.

Infection of Insect Cells—Sf9 cells were grown overnight and infected at a cell density of 3 $\times$ 10^6 cells/ml with the desired viral stocks (MOI = 10). After 1 h of incubation at 27 °C, cell suspension was diluted with InsectXpress supplemented with 5% FBS to 1.5 $\times$ 10^6 cells/ml. 3 days post-infection, cells were controlled for signs of infection and harvested by centrifugation at 500 $\times$ g for 20 min at 4 °C. After washing the cells with PBS, the cell pellet was stored at −80 °C.

Purification of P$_4$-ATPase/CDC50 Complexes—Sf9 cells expressing ATP8B1, ATP8B1^{D454N}, ATP8B2, ATP8B2^{D425N}, and/or CDC50A were lysed with four rounds of nitrogen cavitation (1500 psi, 20 min, on ice) in lysis buffer (50 mM HEPES-KOH pH 8.0, 100 mM NaCl, 5 mM MgCl$_2$, 250 mM sucrose, 1 mM PMSF, protease inhibitors). Unbroken cells and debris were removed by centrifugation at 3,000 $\times$ g (10 min, 4 °C), and membranes were collected at 100,000 $\times$ g (1 h, 4 °C). Protein concentration was determined using a BCA protein assay (Perbio, Breda, the Netherlands). Proteins of interest were purified as previously described by Lenoir *et al.* (39) in the presence of 0.2 mg/ml of either DOPC/DOPA (9:1) or DOPC/DOPA/DOPS (7:1:2). Briefly, membranes were resuspended to 2 mg of membrane protein/ml in 5 ml of solubilization buffer (50 mM HEPES-KOH pH 8.0, 100 mM NaCl, 5 mM MgCl$_2$, 20% glycerol, 0.5% digitonin, 1 mM PMSF, protease inhibitors) and gently shaken at 4 °C for 2 h. Insoluble fraction was pelleted by a 100,000 $\times$ g spin (1 h, 4 °C). Under gentle agitation, detergent-solubilized material was incubated with 100 μl of pre-equilibrated Ni^{2+}-NTA beads (Qiagen) per mg of membrane protein for 2 h at 4 °C. The beads were transferred to a column and washed with 40 volumes of washing buffer 1 (50 mM HEPES-KOH pH 7.2, 200 mM NaCl, 5 mM MgCl$_2$, 20% glycerol, 10 mM imidazole, 0.05% digitonin, 0.2 mg/ml lipids) and 30 volumes of washing buffer 2 (50 mM HEPES-KOH pH 7.2, 100 mM NaCl, 5 mM MgCl$_2$, 20% glycerol, 25 mM imidazole, 0.05% digitonin, 0.2 mg/ml lipids). Proteins were eluted in 5 fractions of 400 μl of elution buffer (50 mM HEPES-KOH pH 7.2, 10 mM NaCl, 5 mM MgCl$_2$, 20% glycerol, 250 mM imidazole, 0.05% digitonin, 0.2 mg/ml lipids), snap-frozen in liquid nitrogen and stored at −80 °C. Purification fractions were subjected to SDS-PAGE and subsequent immunoblotting using mouse anti-HA (12CA5, Santa Cruz) and mouse anti-V5 (Invitrogen) antibodies. The amount of affinity-purified P$_4$-ATPase was estimated by silver staining using purified Ca^{2+}-ATPase derived from rabbit muscle sarcoplasmic reticulum as a reference.

Phosphorylation Assay—^{32}P labeling of purified Ca^{2+}-ATPase was carried out as previously described (39). Affinity-purified P$_4$-ATPase/CDC50 protein complexes were preincubated with 1 mg/ml of desired lipid mixture at 4 °C for 1 h under gentle agitation. For [γ-^{32}P]ATP labeling, ~6 ng of affinity-purified P$_4$-ATPase were incubated at 4 °C for 30 s with 0.2 μM [γ-^{32}P]ATP (5 mCi/μmol) in 150 μl of phosphorylation buffer (50 mM MOPS/Tris pH 7.0, 100 mM KCl, 5 mM MgCl$_2$, 0.05% digitonin, 6 units/ml pyruvate kinase) in the presence or absence of 200 μM orthovanadate. Dephosphorylation was initiated at 20 °C by addition of 5 mM ATP or ADP. Phosphorylation reactions were stopped by acid quenching with ice-cold 16% trichloroacetic acid (TCA) supplemented with 5 mM H$_3$PO$_4$. After a 30 min incubation on ice, protein precipitates were collected at 18,000 $\times$ g (25 min,
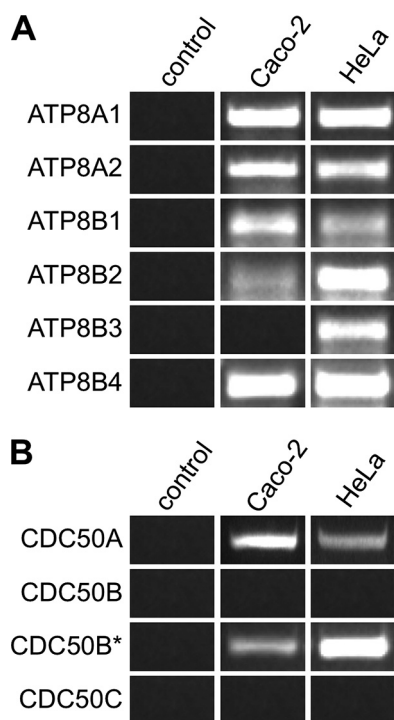
A

B

FIGURE 1. **Expression of class-1 P$_4$-ATPase and CDC50 transcripts in human Caco-2 and HeLa cells.** RT-PCR was performed on total RNA isolated from Caco-2 and HeLa cells. RNA was omitted in control reactions. Primers used are described in Table 1. CDC50B primers were verified using genomic DNA as template (CDC50B*). Sizes of expected and detected mRNA-derived DNA amplification products are as follows: ATP8A1 476 bp, ATP8A2 481 bp, ATP8B1 300 bp, ATP8B2 237 bp, ATP8B3 385 bp, ATP8B4 525 bp, CDC50A 1094 bp, CDC50B 442 bp, CDC50B* 971 bp, CDC50C 555 bp.

4 °C), washed with 800 μl of 7% TCA containing 0.5 mM H$_3$PO$_4$ and incubated on ice for 30 min. The TCA solution was carefully removed after two subsequent centrifugation steps of 18,000 $\times$ g (25 and 10 min, 4 °C), and the pellets were resuspended in SDS sample buffer (150 mM TrisHCl pH 6.8, 10 mM EDTA, 2% SDS, 16% glycerol, 0.025% bromphenol blue, and 5% β-mercaptoethanol) by shaking at 25 °C for 30 min. Aliquots were analyzed by SDS-PAGE following the method of Sarkadi (47). An Imaging Plate (Fujifilm, Steenbergen, the Netherlands) was exposed for 1–5 days to the Coomassie Blue R250-stained and dried SDS gels. Radioactive phosphorylation was detected by a Storm 860 PhosphorImager and quantified against known amounts of [γ-^{32}P]ATP. Samples were corrected for variations in protein precipitation by quantification of Coomassie Blue R250-stained pyruvate kinase.

RESULTS

Expression of Class-1 P$_4$-ATPases and CDC50 Proteins in Human Cell Lines—To systematically investigate interactions between human P$_4$-ATPases and CDC50 proteins, we first analyzed their endogenous expression in human HeLa cervical carcinoma and Caco-2 intestinal carcinoma cells. For P$_4$-ATPases we focused on the six members of the ATP8 or class-1 cluster, *i.e.* ATP8A1, ATP8A2, ATP8B1, ATP8B2, ATP8B3, and ATP8B4. RT-PCR analysis revealed the presence of mRNA for all six ATPases in HeLa cells, and for all except ATP8B3 in Caco-2 cells (Fig. 1A). Remarkably, both

cell types contained mRNA for CDC50A, but lacked any detectable amount of mRNA for the other two CDC50 family members, CDC50B and CDC50C (Fig. 1B). This indicates that HeLa and Caco-2 cells each contain CDC50A as the only putative P$_4$-ATPase interaction partner.

Subcellular Localization of Human Class-1 P$_4$-ATPases and CDC50 Proteins—ATP8B1 and its binding partner CDC50A are localized at the apical membrane of hepatocytes and intestinal epithelial cells (38, 42, 43). The localization of other human class-1 P$_4$-ATPases and CDC50 family members has not been established yet. We therefore analyzed the subcellular distribution of epitope-tagged versions of these proteins in transiently transfected HeLa cells. Confocal immunofluorescence microscopy showed that HA-tagged ATP8B1, ATP8B2, and ATP8B4 localize primarily at the plasma membrane (Fig. 2A). HA-tagged ATP8A1, on the other hand, displayed a perinuclear staining and co-localized with the Golgi marker formiminotransferase-cyclodeaminase (FTCD), indicating that this enzyme resides in the Golgi complex. When expressed at very high levels, these P$_4$-ATPases also showed a nuclear-envelope and reticular staining that coincided with the ER marker protein disulfide isomerase (PDI; Fig. 2A, ATP8B4-HA-positive cell marked with an *asterisk*). When expressed at moderate levels, V5-tagged CDC50A and CDC50B each localized mainly at the plasma membrane (Fig. 2B). In contrast, V5-tagged CDC50C was never found at the plasma membrane and localized exclusively in the ER and perinuclear region.

CDC50 Proteins Are Common Binding Partners of Human Class-1 P$_4$-ATPases—To directly test for physical interactions between human class-1 P$_4$-ATPases and CDC50 proteins, we next performed immunoprecipitation studies on HeLa cells transiently transfected with different combinations of HA-tagged P$_4$-ATPase and V5-tagged CDC50 expression constructs. Expression of tagged protein was verified by immunoblotting of total cell membranes (Fig. 3A). Digitonin-solubilized membranes were used to immunoprecipitate V5-tagged CDC50 proteins with anti-V5 agarose and immunoprecipitates were then analyzed for the presence of HA-tagged P$_4$-ATPases by immunoblotting. ATP8B1-HA was undetectable in immunoprecipitates of cells expressing ATP8B1-HA in the absence of V5-tagged CDC50 proteins. However, co-expression of ATP8B1-HA with either CDC50A-V5 or CDC50B-V5 resulted in co-immunoprecipitation of ATP8B1-HA (Fig. 3B). The immunoprecipitates were devoid of ATP1A1, the catalytic α-subunit of the plasma membrane-associated Na$^+$/K$^+$-ATPase. These results indicate that ATP8B1 interacts directly and specifically with both CDC50A and CDC50B, in agreement with a previous study (38). Immunoprecipitation analysis of ATP8B2, ATP8B4 and ATP8A1 showed that all three enzymes physically interact with both CDC50 subunits. Together, these results indicate that CDC50 proteins are common binding partners of human class-1 P$_4$-ATPases.

From the immunoblots of the total cell lysates, we noticed a remarkable correlation between expression levels of epitopetagged P$_4$-ATPases and CDC50 proteins. In particular, cotransfection of cells with CDC50B-V5 increased expression
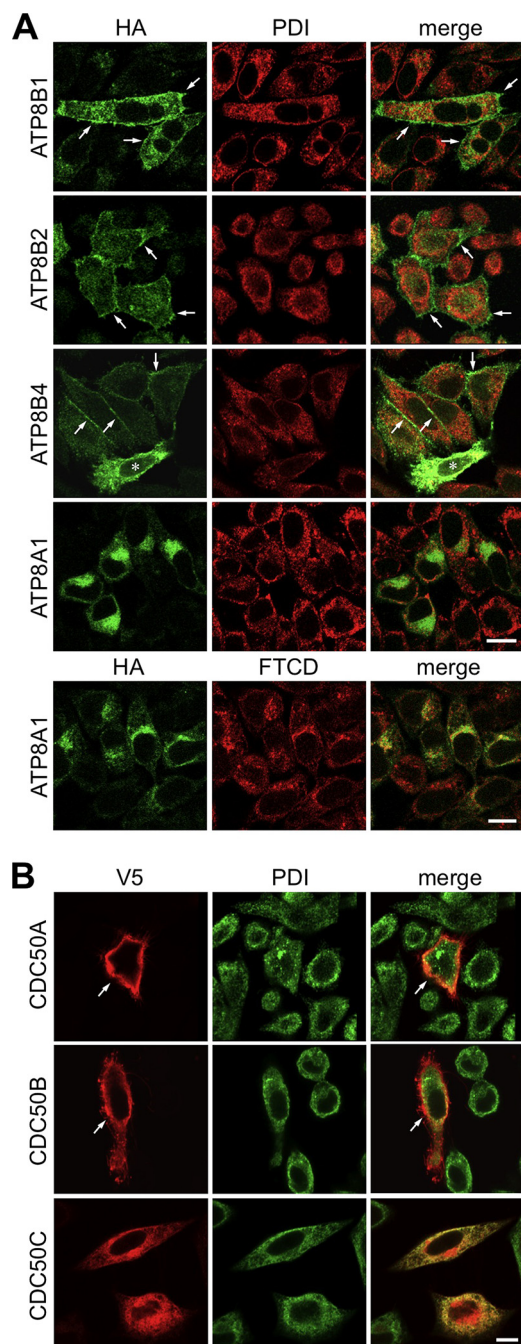
FIGURE 2. **Subcellular localization of human class-1 P$_4$-ATPases and CDC50 proteins in HeLa cells.** *A*, confocal microscopy projections of HeLa cells expressing HA-tagged human P$_4$-ATPases and immunostained with antibodies against HA, the ER-marker PDI and the Golgi-marker FTCD. When expressed at a very high level, HA-tagged P$_4$-ATPases accumulate in the ER (cell marked with *asterisk*). *B*, confocal microscopy projections of HeLa cells expressing V5-tagged human CDC50A, human CDC50B, and macaque CDC50C and immunostained with antibodies against V5 and PDI. *Arrows* indicate sites of clear plasma membrane staining. *Bars*, 10 μm.

levels of all four P$_4$-ATPases relative to their expression levels in CDC50A-V5 transfected or untransfected cells (Fig. 3*A*). This suggests that, even though CDC50B is not a natural binding partner of class-1 P$_4$-ATPases in HeLa cells, its physical interaction with these enzymes has functional consequences.
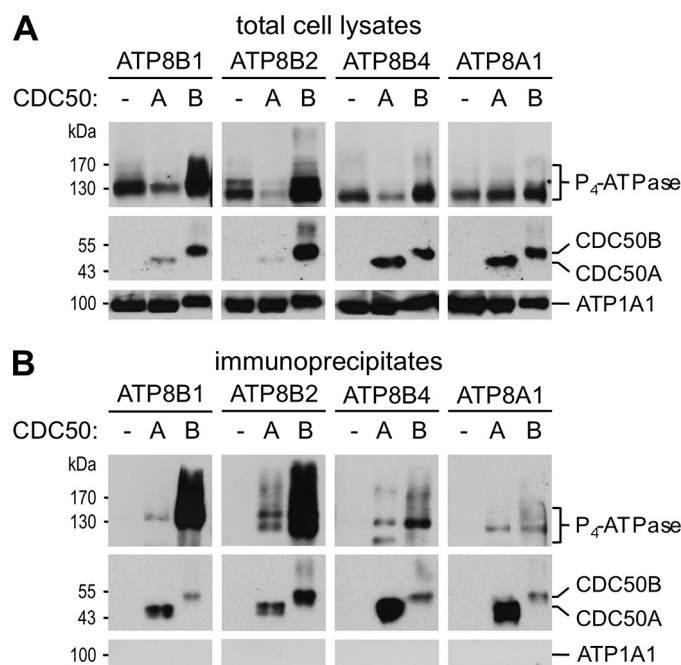

FIGURE 3. **Human CDC50 proteins physically interact with multiple human class-1 P$_4$-ATPases.** HeLa cells co-expressing combinations of HA-tagged P$_4$-ATPases and V5-tagged CDC50 proteins were lysed, extracted with digitonin, and subjected to immunoprecipitation using anti-V5 antibody-loaded agarose beads. Total cell lysates (*A*) and immunoprecipitates (*B*) were analyzed by immunoblotting using antibodies against HA, V5 and the plasma membrane-associated Na$^+$/K$^+$-ATPase α-subunit ATP1A1. HeLa cells expressing HA-tagged P$_4$-ATPases in the absence of V5-tagged CDC50 proteins were used as control (−). Because expression levels of CDC50B were generally much higher than for CDC50A, the corresponding samples were 50-fold diluted prior to immunoblot analysis with the anti-V5 antibody.

CDC50 Proteins Are Required for Export of Human Class-1 P$_4$-ATPases from the ER—P$_4$-ATPase/CDC50 complex formation in yeast is essential for P$_4$-ATPase export from the ER (32, 33). Moreover, co-expression of CDC50A or CDC50B is needed to direct ATP8B1 from the ER to the plasma membrane in CHO-derived UPS-1 cells (38). In view of the foregoing localization studies in HeLa cells, it is possible that the endogenous levels of CDC50 proteins in UPS-1 cells fall short to enable plasma membrane delivery of heterologously expressed ATP8B1. To investigate whether human class-1 P$_4$-ATPases in general rely on CDC50 proteins for ER export, different combinations of red fluorescent protein (RFP)-tagged P$_4$-ATPases and V5-tagged CDC50 proteins were expressed in UPS-1 cells and their subcellular distributions were examined by confocal fluorescence microscopy. RFP-tagged ATP8B1, ATP8B2, ATP8B4, and ATP8A1 expressed in UPS-1 cells did not reach the plasma membrane and accumulated in the ER (Fig. 4, *controls*). When co-expressed with CDC50A-V5 or CDC50B-V5, a substantial portion of ATP8B1-RFP was found at the plasma membrane (Fig. 4*A*). Likewise, co-expression of CDC50A-V5 or CDC50B-V5 shifted the localization of RFP-tagged ATP8B2, ATP8B4, and ATP8A1 from the ER to the plasma membrane (Fig. 4, *B–D*). The plasma membrane delivery of ATP8A1 in CDC50-expressing UPS-1 cells was unexpected, given that this enzyme primarily localizes to the Golgi in HeLa cells (Fig. 2*A*). Why UPS-1 cells are unable to retain ATP8A1 in the Golgi remains
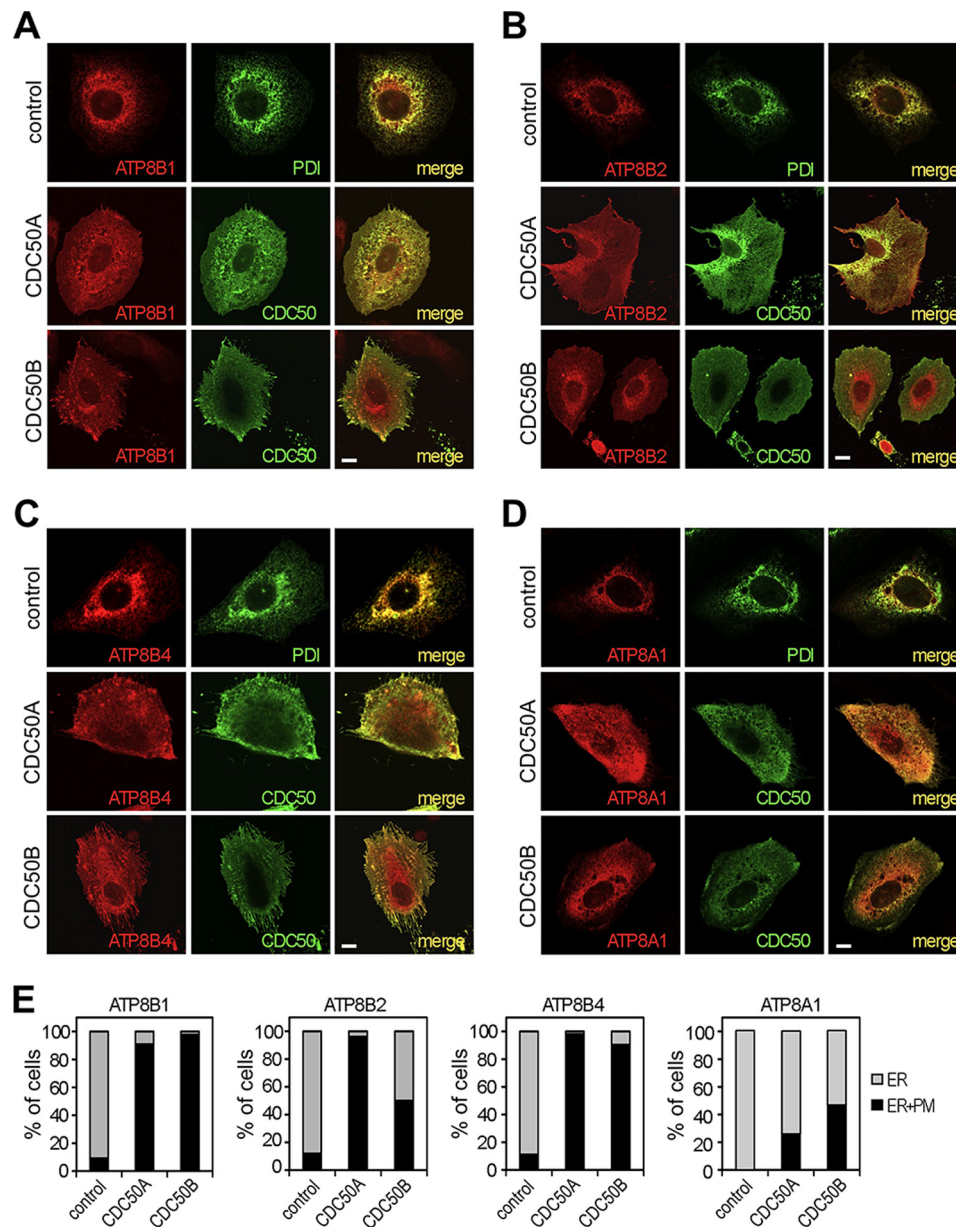
FIGURE 4. **Human P$_4$-ATPases require CDC50 proteins for ER export.** Confocal microscopy projections of CHO-K1 derived UPS-1 cells expressing RFP-tagged ATP8B1 (*A*), ATP8B2 (*B*), ATP8B4 (*C*), and ATP8A1 (*D*) in the presence or absence of V5-tagged CDC50A or CDC50B. Cells were immunostained with antibodies against V5 and the ER marker PDI. For each sample, a representative picture is shown. Bar, 10 μm. *E*, quantification of CDC50-dependent redistribution of P$_4$-ATPases in UPS-1 cells. For each condition, more than two hundred cells were examined and categorized as ER if the RFP-tagged P$_4$-ATPase was fully retained in the ER or as ER + PM in case a substantial portion of the RFP-tagged P$_4$-ATPase localized at the plasma membrane.

to be established. In any case, the CDC50-mediated redistribution of P$_4$-ATPases in UPS-1 cells was highly reproducible (Fig. 4*E*) and independent of the transport competence of these enzymes, since a considerable fraction of catalytically dead mutants of ATP8B1 and ATP8B2 (*i.e.* ATP8B1^{D454N} and ATP8B2^{D425N}) still reached the plasma membrane when co-expressed with CDC50A-V5 or CDC50B-V5 (Fig. 5). Hence, rather than being a unique property of ATP8B1, requirement of a CDC50 subunit for ER export is a widespread feature among human class-1 P$_4$-ATPases.

Purification of Human Class-1 P$_4$-ATPase/CDC50 Complexes—Co-expression of ATP8B1 with CDC50A or CDC50B has been shown to restore NBD-PS transport at the plasma membrane of PS transport-defective UPS-1 cells,

while expression of ATP8B1 alone had no effect (38). Whether CDC50 proteins are directly involved in ATP8B1-catalyzed lipid transport and serve a role beyond facilitating ER export of the enzyme is not known. This led us to analyze the catalytic activity of ATP8B1 and ATP8B2 purified from baculovirus-infected insect cells in the absence or presence of a CDC50 binding partner. Co-expression was achieved by co-infecting insect cells with two recombinant viruses, one for expression of polyhistidine and HA-tagged ATP8B1, or ATP8B2, and the other one for expression of V5-tagged CDC50A. Attempts to create stable viral stocks for heterologous expression of V5-tagged CDC50B were unsuccessful. Heterologous expression of the tagged proteins was verified by immunoblotting (data not shown). Crude membranes pre-
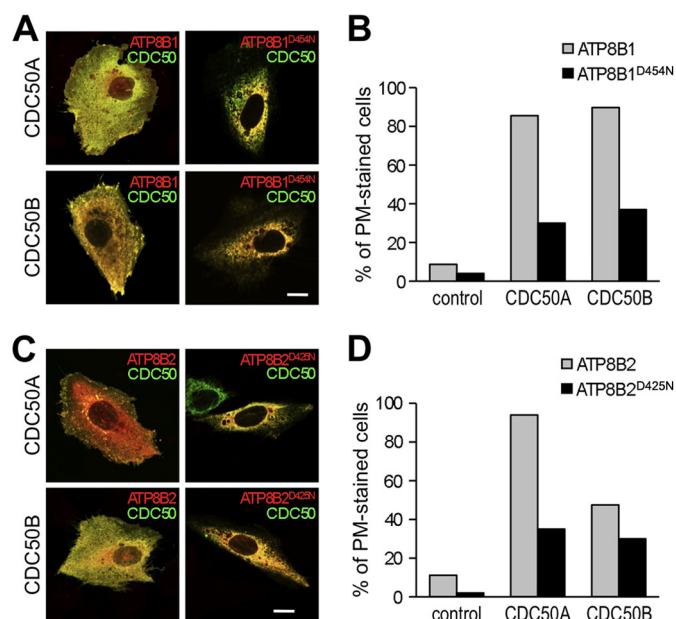
FIGURE 5. **Human P_4-ATPases and their catalytically inactive aspartate mutants depend on CDC50 proteins for ER export.** Confocal microscopy projections of CHO-K1-derived UPS-1 cells expressing RFP-tagged ATP8B1 or ATP8B1^{D454N} (*A*) as well as ATP8B2 or ATP8B2^{D425N} (*B*) in the presence of V5-tagged CDC50A or CDC50B. Cells were immunostained with antibodies raised against V5 and the ER marker PDI. For each condition, a representative picture is displayed. Bar, 10 μm. *C* and *D*, quantification of CDC50-dependent redistribution of P_4-ATPases and their enzymatically inactive aspartate mutants in UPS-1 cells. For each sample, more than 200 double-transfected cells were examined and categorized by presence or absence of P_4-ATPase-derived PM staining.

pared from infected insect cells were solubilized using digitonin. The extracts were subjected to Ni^{2+}-NTA affinity chromatography. Fig. 6*A* shows the Ni^{2+}-NTA elution profiles of ATP8B1 expressed alone (*left panel*) or in combination with CDC50A (*right panel*). Similar Ni^{2+}-NTA elution profiles were obtained for ATP8B2. The presence of stable ATP8B1-CDC50A and ATP8B2-CDC50A complexes in the eluates was verified by co-immunoprecipitation analysis using anti-V5 agarose (data not shown). Peak fractions were pooled and analyzed for P_4-ATPase-mediated catalytic activity, as described below.

Phosphoenzyme Formation of Human Class-1 P_4-ATPases ATP8B1 and ATP8B2 Requires a CDC50 Binding Partner—An essential step in the reaction cycle of P-type ATPases is formation of an acid-stable, phosphorylated Asp residue. Formation of this phosphoenzyme intermediate requires ATP and is blocked by orthovanadate (VO_4), a potent inhibitor of P-type ATPases (44). To investigate whether ATP8B1 is able to form a phosphoenzyme intermediate *in vitro*, the affinity-purified protein was incubated with [γ-^{32}P]ATP at 4 °C, run on a gel and analyzed by autoradiography. Because the presence of aminophospholipid substrate is expected to stimulate dephosphorylation of the phosphoenzyme intermediate (31, 45), endogenous phospholipid was removed by washing the Ni^{2+}-NTA-bound P_4-ATPases extensively in buffer containing 0.05% digitonin and 0.2 mg/ml of nonsubstrate phospholipids phosphatidylcholine and phosphatidic acid.

When purified in the absence of its binding partner CDC50A, ATP8B1 was unable to form a VO_4-sensitive phos-

phoenzyme intermediate (Fig. 6, *B* and *C*). This was also the case when incubations were performed at an elevated temperature (30 °C) and/or in the presence of the putative phospholipid substrate PS (Fig. 7*B*, data not shown). In contrast, ATP8B1 purified as a complex with CDC50A readily formed a VO_4-sensitive phosphoenzyme intermediate. Formation of this intermediate was completely blocked by mutation of the catalytically important Asp residue at position 454 (D454N, Fig. 6, *B* and *C*). Hence, formation of the phosphoenzyme intermediate of ATP8B1 is critically dependent on its CDC50 binding partner.

Phosphorylation of ATP8B1 in the presence of CDC50A reached a maximum within 5 s after addition of [γ-^{32}P]ATP at 4 °C (Fig. 7*B*). This rate of phosphorylation was very similar to that observed for the P-type Ca^{2+}-pump SERCA in muscle sarcoplasmic vesicles in the presence of Ca^{2+} (Fig. 7*A*). The stoichiometry of phosphorylation for ATP8B1 was 10-fold lower than that for SERCA (10 mmol/mol *versus* 100 mmol/mol enzyme, respectively). This is not unexpected considering that the enzymatic activity of ATP8B1 was analyzed in detergent extracts rather than in its native membrane environment. Binding of phospholipid substrate would be required for P_4-ATPases to dephosphorylate, analogous to the role of protons in dephosphorylation of SERCA (31). Addition of excess cold ATP triggered a fast ($t_{1/2} < 2$ s) and complete release of ^{32}P from the phosphoenzyme intermediate of SERCA (Fig. 7*A*). In contrast, only a minor fraction (maximum 10%) of the phosphoenzyme intermediate of ATP8B1 could be dephosphorylated in the presence of cold ATP, even if the incubation mixtures contained PS, which would be essential to complete this step (Fig. 7*C*). Hence, the bulk of ATP8B1 molecules associated with CDC50A is unable to progress through the reaction cycle.

P-type ATPases normally undergo a conformational transition from a high energy *E*1P to a lower energy *E*2P form (31). Although the *E*1P form can readily undergo back reaction with ADP to reform ATP, the *E*2P form can no longer transfer the enzyme-bound phosphate back to ADP. As shown in Fig. 7*C*, CDC50A-associated ATP8B1 could not react with ADP. This indicates that the bulk of the ATP8B1-CDC50A complex entering the reaction cycle is readily processed from *E*1 to *E*1P and from *E*1P to *E*2P, but then gets stuck at the *E*2P stage. In line with this observation, the Ni^{2+}-NTA fractions used for the phosphorylation assays did not contain any ATPase activity that could be traced back to ATP8B1 (Fig. 8). Hence, although ATP8B1 associated with CDC50A is capable of phosphoenzyme formation, CDC50A binding by itself is not sufficient to allow subsequent dephosphorylation of the enzyme, even in the presence of its putative substrate, PS.

We next investigated whether the requirement of a CDC50 subunit for phosphorylation of ATP8B1 extends to other human class-1 P_4-ATPases. ATP8B2 purified as a complex with CDC50A readily formed a VO_4-sensitive phosphoenzyme intermediate, although the stoichiometry of phosphorylation (0.4 mmol/mol of enzyme) was substantially lower than that of ATP8B1 when associated with CDC50A (10 mmol/mol of enzyme; Fig. 6, *C–E*). The reason for this is unclear. Nonetheless, as observed for ATP8B1, formation of the phosphoen-
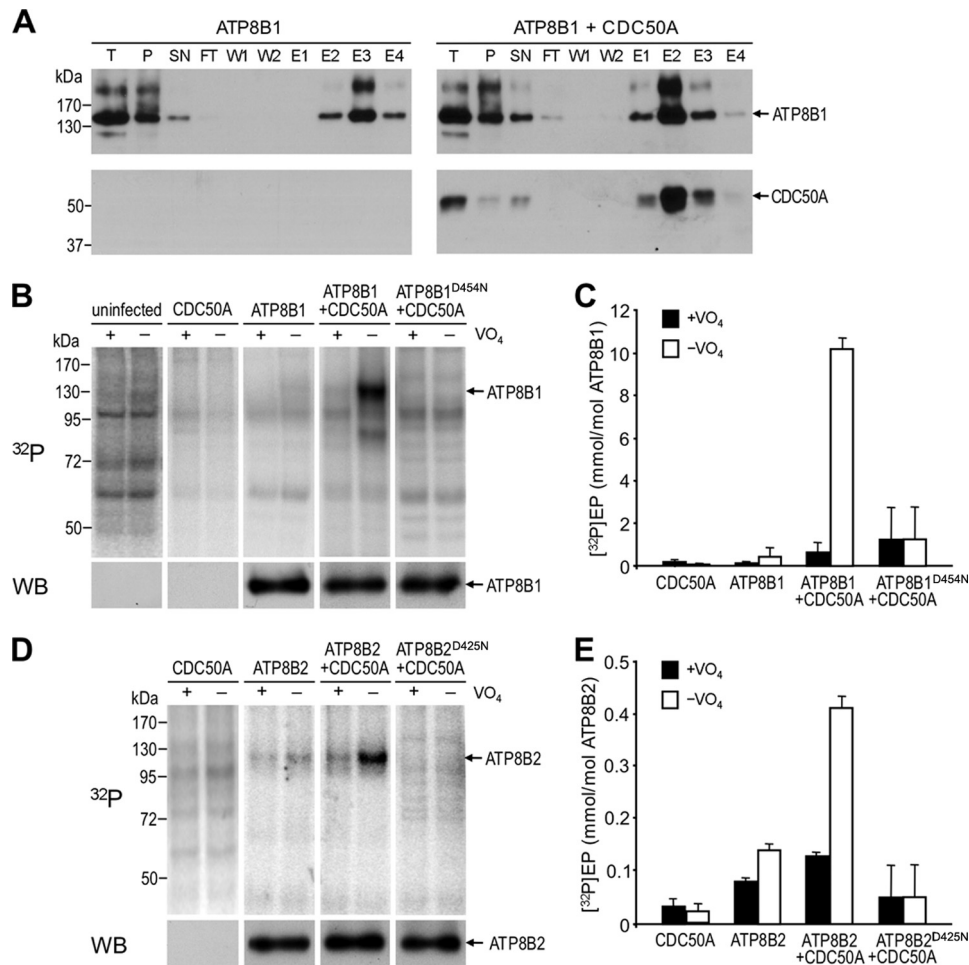
FIGURE 6. **ATP8B1 and ATP8B2 phosphoenzyme formation is strictly dependent on CDC50 proteins.** *A*, digitonin-solubilized membranes prepared from baculovirus-infected insect cells expressing HA$_3$/polyHis-tagged ATP8B1 alone (*left*) or in combination with V5-tagged CDC50A (*right*) were subjected to Ni^{2+}-NTA-affinity chromatography and immunoblot analysis using anti-HA (*top*) and anti-V5 antibodies (*bottom*). The following fractions were loaded onto a 10% SDS-PAGE gel for immunoblotting: *T*, total membranes; *P*, insoluble membrane fraction; *SN*, soluble membrane fraction; *FT*, flow-through; *W1-2*, wash 1–2; *E1–4*, eluate fractions 1–4. *B*, ATP8B1 was affinity-purified from baculovirus-infected insect cells expressing ATP8B1 alone or in combination with CDC50A, and then labeled with [γ-^{32}P]ATP for 30 s at 4 °C in the absence or presence of 200 μM orthovanadate (VO$_4$). Phosphoenzyme formation was detected by autoradiography (^{32}P) and quantified for the same amount of protein as determined by immunoblotting (*WB*) using anti-HA antibody. Uninfected insect cells or infected cells expressing CDC50A alone or in combination with the enzyme-dead ATP8B1^{D454N} mutant served as controls. *C*, quantification of results presented in *B*. Data shown are means ± S.D. of three independent experiments. *D*, [γ-^{32}P]ATP labeling of affinity-purified ATP8B2 as described for ATP8B1. Baculovirus-infected insect cells expressing CDC50A alone or in combination with the enzyme-dead ATP8B2^{D425N} mutant served as controls. *E*, quantification of results presented in *D*. Data shown are means ± range of two independent experiments.

zyme intermediate of ATP8B2 was strictly dependent on the presence of CDC50A (Fig. 6, *D* and *E*). Collectively, these findings support an essential role of CDC50 proteins in the reaction cycle of human class-1 P$_4$-ATPases.

DISCUSSION

P$_4$-ATPases are required for phospholipid transport and asymmetry, but it is unclear whether these enzymes alone are sufficient to translocate phospholipids. At least some P$_4$-ATPases form heteromeric complexes with CDC50 protein family members and previous work in yeast provided evidence that these accessory proteins play a critical role in the P$_4$-ATPase transport reaction (31). The human genome encodes surprisingly few CDC50 homologues given the large number of different human P$_4$-ATPases (40). This led us to initiate a systematic analysis of the physical and functional interactions between human members of these two protein families. We found that human CDC50A and CDC50B proteins can each

form heteromeric complexes with multiple human class-1 P$_4$-ATPases, and that in all cases examined association with a CDC50 homologue is needed for P$_4$-ATPase export from the ER. Moreover, we demonstrate that phosphorylation of the catalytically important Asp residue in class-1 P$_4$-ATPases ATP8B1 and ATP8B2 is strictly dependent on their association with a CDC50 subunit. Collectively, these results suggest that CDC50 proteins are integral part of the mechanism by which P$_4$-ATPase translocate phospholipids.

Previous work revealed that ATP8B1 requires either CDC50A or CDC50B for ER exit and delivery to the plasma membrane in CHO-derived UPS-1 cells (38). We now extend these observations by showing that ATP8A1, ATP8B2, and ATP8B4 also rely on association with a CDC50 binding partner to reach their post-ER destinations. The promiscuous interactions observed between human P$_4$-ATPases and CDC50 proteins are striking, given that in yeast the plasma
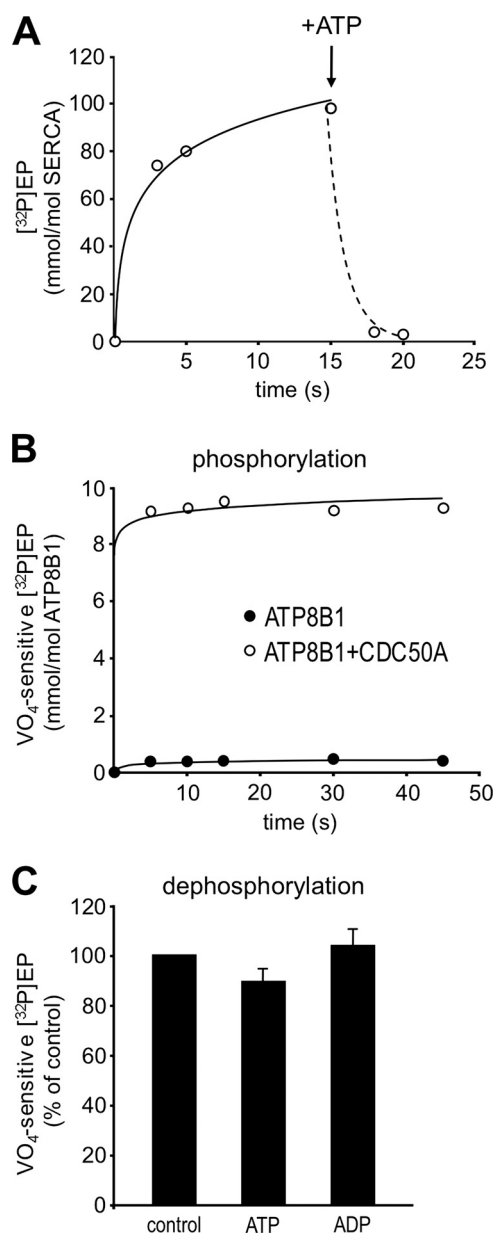
A

B phosphorylation

● ATP8B1
○ ATP8B1+CDC50A

C dephosphorylation

FIGURE 7. **The phosphorylation-competent ATP8B1/CDC50A complex is trapped in the *E*2P conformation.** *A*, sarcoplasmic reticular vesicles were labeled with 2 μM [γ-^{32}P]ATP at 4 °C for various time periods in the presence of 20 μM CaCl$_2$ (*solid line*). Samples ^{32}P-labeled for 3 or 5 s with 5 mM ATP to trigger dephosphorylation (*dashed line*). Phosphoenzyme formation was detected by subsequent autoradiography. *B*, membranes derived from baculovirus-infected insect cells expressing either HA$_3$His$_{10}$-tagged ATP8B1 alone or in combination with V5-tagged CDC50A were digitonin-solubilized and subjected to Ni^{2+}-NTA-affinity chromatography. Proteins of interest were purified in the presence of exogenous DOPC/DOPA/DOPS (7:1:2) and phosphorylated at 4 °C in the presence or absence of 200 μM VO$_4$. *C*, following ^{32}P-labeling for 45 s, dephosphorylation of ATP8B1 co-purified with CDC50A in the presence of DOPC/DOPA/DOPS (7:1:2) was stimulated at 20 °C for 30 s by addition of 5 mM ATP or 5 mM ADP. Data shown are means ± range of two independent experiments.

membrane and Golgi-resident P$_4$-ATPases Dnf1/2p, Dnf3p, and Drs2p each rely on association with a different CDC50 subunit for export from the ER (32, 33). Recent studies in *Arabidopsis* indicate that any potential sorting information associated with the CDC50 subunits is dominated by P$_4$-ATPase-encoded signals (36). Moreover, the various plant
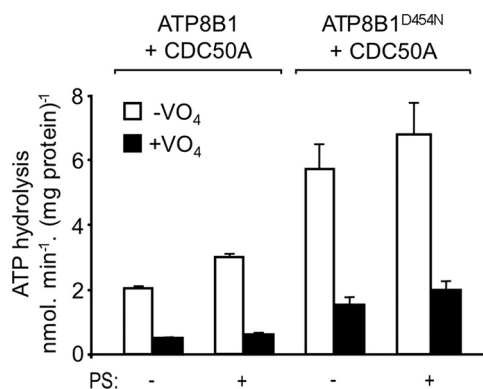

FIGURE 8. **ATPase activity of fractions containing ATP8B1 and ATP8B1^{D454N} affinity-purified in the presence of CDC50A.** Membranes derived from baculovirus-infected insect cells expressing V5-tagged CDC50A in combination with either HA$_3$His$_{10}$-tagged ATP8B1 or ATP8B1^{D454N} were digitonin-solubilized and subjected to Ni^{2+}-NTA-affinity chromatography. Affinity purification was carried out in the absence (−PS: PC/PA, 9:1) or presence of PS (+PS: PC/PA/PS, 7:1:2). The rate of ATP hydrolysis in fractions containing affinity-purified protein was determined by a phosphomolybdate colorimetric assay using the amount of P$_i$ liberated within 30–120 min at 30 °C in the absence or presence of VO$_4$. Note that the fraction containing affinity-purified ATP8B1 in which the catalytically important Asp residue is mutated to Asn (D454N) still shows a prominent ATPase activity, indicating that this activity is unrelated to ATP8B1. The identity of the contaminating enzyme remains to be established.

P$_4$-ATPases gain functionality when co-expressed with any of three different CDC50 proteins, but retain their different lipid substrate specificities independently of the nature of the CDC50 binding partner (36). While these studies indicate that sorting information and substrate determinants primarily reside in the P$_4$-ATPase, they do not address the primary role of the CDC50 polypeptide in the transporter complex.

We previously reported that phosphorylation of the catalytically important Asp residue in the yeast P$_4$-ATPase Drs2p relies on direct and specific interactions with its Cdc50p subunit (39). Indeed, a role of Cdc50p in the catalytic cycle of Drs2p may explain the suboptimal flippase activity detected in proteoliposomes containing affinity-purified Drs2p and substoichiometric amounts of Cdc50p (22). We now find that human class-1 P$_4$-ATPases ATP8B1 and ATP8B2 also require association with a CDC50 subunit to form a phosphoenzyme intermediate. Collectively, these results provide further support for the notion that CDC50 proteins are vital components of the P$_4$-ATPase transport machinery. However, this concept is at odds with another study reporting that the murine class-1 P$_4$-ATPase Atp8a1 purified from baculovirus-infected insect cells retains PS-specific ATPase activity in the absence of any native CDC50 binding partner (48). This implies that Atp8a1, contrary to ATP8B1 and ATP8B2, is capable of forming a functional complex with CDC50 proteins endogenously expressed in insect cells or, alternatively, that this enzyme may act on its own. It deserves mention that we and others encountered contaminating ATPase activities in P$_4$-ATPase/CDC50 complex-containing eluates that appeared devoid of other proteins (Refs. 22 and 39, Fig. 8). These contaminating activities came to light when using an inactive P$_4$-ATPase mutant as control. Because such control was missing in the study on Atp8a1, additional work will be necessary to determine whether or not this enzyme requires a CDC50 binding partner for catalytic activity.

Our present findings raise the question of how CDC50 proteins would render P$_4$-ATPases competent for phosphorylation of the conserved Asp residue. One possibility is that the subunit is required for conversion of the enzyme from the E1 to the E1P form. However, we show that the phosphorylation reaction is sensitive to vanadate, which is known to act on the E2 form (46). So it is feasible that our assay actually measures the fraction of ATPase molecules that corresponds to or can reach the E2 form of the enzyme, which then can proceed to the phosphorylation reaction. Therefore, our data do not exclude a role of the subunit in the E2P to E2 transition. In fact, such a role is consistent with our finding that the affinity of Drs2p for Cdc50p fluctuates during the reaction cycle, with the strongest interaction occurring between the subunit and E2P conformation of the enzyme (39). Efforts to distinguish between the above possibilities are hampered by the fact that the bulk of purified ATP8B1 molecules that can form a phosphoenzyme intermediate cannot continue successfully through the remainder of the reaction cycle, but gets stuck at the E2P step. In fact, this was also observed for Drs2p purified from yeast (39). As the fraction capable of dephosphorylation is not substantially increased in the presence of PS, the problem is not the absence of transportable phospholipid substrate. It is feasible that loading of phospholipid substrate is perturbed by the presence of detergent. Another possibility is that the phosphorylated form of the enzyme is missing another component required to continue through the cycle. In this respect, it is of interest to note that catalytic activity of Drs2p is subject to regulation by phosphoinositides (49). Consequently, additional work will be necessary to elucidate the precise contribution of CDC50 proteins to the P$_4$-ATPases reaction cycle.

In sum, our studies suggest that CDC50 proteins are indispensable components of the P$_4$-ATPase transport machinery. Thus, acquisition of CDC50 subunits may have been a crucial step in how the basic transport mechanism of P-type cation pumps was adapted to execute translocation of phospholipids. The finding that human P$_4$-ATPase/CDC50 complexes purified from baculovirus-infected insect cells retain enzymatic activity provides an attractive starting point to further dissect the role of CDC50 proteins in P$_4$-ATPase-catalyzed phospholipid transport.

REFERENCES

1. Op den Kamp, J. A. (1979) *Annu. Rev. Biochem.* **48,** 47–71
2. Alder-Baerens, N., Lisman, Q., Luong, L., Pomorski, T., and Holthuis, J. C. (2006) *Mol. Biol. Cell* **17,** 1632–1642
3. van Meer, G., Voelker, D. R., and Feigenson, G. W. (2008) *Nat. Rev. Mol. Cell Biol.* **9,** 112–124
4. Devaux, P. F. (2000) *Biochimie* **82,** 497–509
5. Pomorski, T., Lombardi, R., Riezman, H., Devaux, P. F., van Meer, G., and Holthuis, J. C. (2003) *Mol. Biol. Cell* **14,** 1240–1254
6. Graham, T. R. (2004) *Trends Cell Biol.* **14,** 670–677
7. Kinnunen, P. K., and Holopainen, J. M. (2000) *Biosci. Rep.* **20,** 465–482
8. Balasubramanian, K., and Schroit, A. J. (2003) *Annu. Rev. Physiol.* **65,** 701–734
9. Mercer, J., and Helenius, A. (2008) *Science* **320,** 531–535
10. Devaux, P. F. (1991) *Biochemistry* **30,** 1163–1173
11. Daleke, D. L. (2007) *J. Biol. Chem.* **282,** 821–825
12. Seigneuret, M., and Devaux, P. F. (1984) *Proc. Natl. Acad. Sci. U.S.A.* **81,** 3751–3755
13. Pomorski, T., Herrmann, A., Müller, P., van Meer, G., and Burger, K. (1999) *Biochemistry* **38,** 142–150
14. Natarajan, P., Wang, J., Hua, Z., and Graham, T. R. (2004) *Proc. Natl. Acad. Sci. U.S.A.* **101,** 10614–10619
15. Zachowski, A., Henry, J. P., and Devaux, P. F. (1989) *Nature* **340,** 75–76
16. Tang, X., Halleck, M. S., Schlegel, R. A., and Williamson, P. (1996) *Science* **272,** 1495–1497
17. Gomès, E., Jakobsen, M. K., Axelsen, K. B., Geisler, M., and Palmgren, M. G. (2000) *Plant Cell* **12,** 2441–2454
18. Poulsen, L. R., López-Marqués, R. L., McDowell, S. C., Okkeri, J., Licht, D., Schulz, A., Pomorski, T., Harper, J. F., and Palmgren, M. G. (2008) *Plant Cell* **20,** 658–676
19. Darland-Ransom, M., Wang, X., Sun, C. L., Mapes, J., Gengyo-Ando, K., Mitani, S., and Xue, D. (2008) *Science* **320,** 528–531
20. Wang, L., Beserra, C., and Garbers, D. L. (2004) *Dev. Biol.* **267,** 203–215
21. Paulusma, C. C., Groen, A., Kunne, C., Ho-Mok, K. S., Spijkerboer, A. L., Rudi de Waart, D., Hoek, F. J., Vreeling, H., Hoeben, K. A., van Marle, J., Pawlikowska, L., Bull, L. N., Hofmann, A. F., Knisely, A. S., and Oude Elferink, R. P. (2006) *Hepatology* **44,** 195–204
22. Zhou, X., and Graham, T. R. (2009) *Proc. Natl. Acad. Sci. U.S.A.* **106,** 16586–16591
23. Coleman, J. A., Kwok, M. C., and Molday, R. S. (2009) *J. Biol. Chem.* **284,** 32670–32679
24. Axelsen, K. B., and Palmgren, M. G. (1998) *J. Mol. Evol.* **46,** 84–101
25. Kühlbrandt, W. (2004) *Nat. Rev. Mol. Cell Biol.* **5,** 282–295
26. Toyoshima, C., and Inesi, G. (2004) *Annu. Rev. Biochem.* **73,** 269–292
27. Olesen, C., Picard, M., Winther, A. M., Gyrup, C., Morth, J. P., Oxvig, C., Møller, J. V., and Nissen, P. (2007) *Nature* **450,** 1036–1042
28. Morth, J. P., Pedersen, B. P., Toustrup-Jensen, M. S., Sorensen, T. L., Petersen, J., Andersen, J. P., Vilsen, B., and Nissen, P. (2007) *Nature* **450,** 1043–1049
29. Shinoda, T., Ogawa, H., Cornelius, F., and Toyoshima, C. (2009) *Nature* **459,** 446–450
30. Pedersen, B. P., Buch-Pedersen, M. J., Morth, J. P., Palmgren, M. G., and Nissen, P. (2007) *Nature* **450,** 1111–1114
31. Lenoir, G., Williamson, P., and Holthuis, J. C. (2007) *Curr. Opin. Chem. Biol.* **11,** 654–661
32. Saito, K., Fujimura-Kamada, K., Furuta, N., Kato, U., Umeda, M., and Tanaka, K. (2004) *Mol. Biol. Cell* **15,** 3418–3432
33. Furuta, N., Fujimura-Kamada, K., Saito, K., Yamamoto, T., and Tanaka, K. (2007) *Mol. Biol. Cell* **18,** 295–312
34. Kato, U., Emoto, K., Fredriksson, C., Nakamura, H., Ohta, A., Kobayashi, T., Murakami-Murofushi, K., and Umeda, M. (2002) *J. Biol. Chem.* **277,** 37855–37862
35. Chen, S., Wang, J., Muthusamy, B. P., Liu, K., Zare, S., Andersen, R. J., and Graham, T. R. (2006) *Traffic* **7,** 1503–1517
36. López-Marqués, R. L., Poulsen, L. R., Hanisch, S., Meffert, K., Buch-Pedersen, M. J., Jakobsen, M. K., Pomorski, T. G., and Palmgren, M. G. (2010) *Mol. Biol. Cell* **21,** 791–801
37. Bull, L. N., van Eijk, M. J., Pawlikowska, L., DeYoung, J. A., Juijn, J. A., Liao, M., Klomp, L. W., Lomri, N., Berger, R., Scharschmidt, B. F., Knisely, A. S., Houwen, R. H., and Freimer, N. B. (1998) *Nat. Genet.* **18,** 219–224
38. Paulusma, C. C., Folmer, D. E., Ho-Mok, K. S., de Waart, D. R., Hilarius, P. M., Verhoeven, A. J., and Oude Elferink, R. P. (2008) *Hepatology* **47,** 268–278
39. Lenoir, G., Williamson, P., Puts, C. F., and Holthuis, J. C. (2009) *J. Biol. Chem.* **284,** 17956–17967
40. Paulusma, C. C., and Oude Elferink, R. P. (2005) *Biochim. Biophys. Acta* **1741,** 11–24

41. Katoh, Y., and Katoh, M. (2004) *Oncol. Rep.* **12,** 939–943
42. Eppens, E. F., van Mil, S. W., de Vree, J. M., Mok, K. S., Juijn, J. A., Oude Elferink, R. P., Berger, R., Houwen, R. H., and Klomp, L. W. (2001) *J. Hepatol.* **35,** 436–443
43. van Mil, S. W., van Oort, M. M., van den Berg, I. E., Berger, R., Houwen, R. H., and Klomp, L. W. (2004) *Pediatr. Res.* **56,** 981–987
44. Cantley, L. C., Jr., Cantley, L. G., and Josephson, L. (1978) *J. Biol. Chem.* **253,** 7361–7368
45. Ding, J., Wu, Z., Crider, B. P., Ma, Y., Li, X., Slaughter, C., Gong, L., and Xie, X. S. (2000) *J. Biol. Chem.* **275,** 23378–23386
46. Smith, R. L., Zinn, K., and Cantley, L. C. (1980) *J. Biol. Chem.* **255,** 9852–9859
47. Sarkadi, B., Enyedi, A., Földes-Papp, Z., and Gárdos, G. (1986) *J. Biol. Chem.* **261,** 9552–9557
48. Paterson, J. K., Renkema, K., Burden, L., Halleck, M. S., Schlegel, R. A., Williamson, P., and Daleke, D. L. (2006) *Biochemistry* **45,** 5367–5376
49. Natarajan, P., Liu, K., Patil, D. V., Sciorra, V. A., Jackson, C. L., and Graham, T. R. (2009) *Nat. Cell Biol.* **11,** 1421–1426